

Intense radioactive-ion beams produced with the ISOL method

U. Köster^a

CERN, ISOLDE, CH-1211 Geneva 23, Switzerland

Received: 21 March 2002 /

Published online: 31 October 2002 – © Società Italiana di Fisica / Springer-Verlag 2002

Abstract. For fifty years the isotope separation on-line (ISOL) technique has been used for the production of radioactive-ion beams (RIBs). Thick-target ISOL facilities can provide very intense RIBs for a wide range of applications. The important design parameters for an ISOL facility are efficiency, rapidity and selectivity of all steps of the separation process. To achieve the anticipated beam intensities with the next-generation RIB facilities, the production rate in the ISOL target has to be increased by orders of magnitude. This is only possible by adapting the projectile beam for optimum production cross-sections and simultaneously minimizing the target heating due to the electronic stopping power of charged-particle projectiles. ISOL beams of 75 different elements have been produced up to now and further beam development is under way to produce a still greater variety of isotopes and to improve existing beams in intensity and purity.

PACS. 25.40.Sc Spallation reactions – 25.85.Ec Neutron-induced fission – 25.85.Ge Charged-particle-induced fission – 25.85.Jg Photofission

1 Introduction

Fifty years ago [1], the first radioactive-ion beams (RIBs) were produced with the isotope separation on-line (ISOL) method: the nuclear-reaction products are stopped and neutralized in the target, then diffuse and effuse out and find eventually their way to an attached ion source where they are ionized. The ions are electrostatically accelerated to some ten of keV and mass-separated in a dipole magnet. Nowadays ISOL facilities provide a great variety of mass-, isotope- or even isomer-separated ion beams which can be easily guided to various experimental set-ups serving a multitude of applications [2].

Also other methods have been developed to provide RIBs: namely, in-flight separators and ion-guide ISOL (IGISOL) systems, a variant in which the reaction products are not stopped in a solid catcher, but in a gas cell. Finally, there are also the chemical separators, indeed the oldest method to separate and identify radioactive isotopes. This article gives a review of basics and recent developments of the ISOL technique together with comparisons to the other separation methods where appropriate.

2 Factors determining the RIB intensity

The decisive figure of merit for any RIB facility is the intensity and purity of its beams. For an ISOL facility the

beam intensity provided to the user is given by¹

$$i = \Phi \cdot \sigma \cdot N \cdot \varepsilon_{\text{target}} \cdot \varepsilon_{\text{source}} \cdot \varepsilon_{\text{sep}} \cdot \varepsilon_{\text{transp}} \quad (1)$$

The production in the target is determined by $\Phi \cdot \sigma \cdot N$, *i.e.* the flux of primary particles, the cross-section to produce the desired isotope and the number of target atoms exposed to the primary beam. One obtains the usable RIB intensity by multiplying with the release efficiency from the target $\varepsilon_{\text{target}}$, the ion source efficiency $\varepsilon_{\text{source}}$, the transmission of the mass separator ε_{sep} and the transmission to the user set-up $\varepsilon_{\text{transp}}$. Note that the decay losses are included in the individual efficiencies ε_{\dots} which depend thus on the rapidity of release and transport and the lifetime of the isotope under consideration. The selectivity of the separation is another important parameter. With a less selective method the isobaric background will be higher and more data must be collected to obtain a significant signal above background for an exotic isotope. In the worst case it becomes impossible to detect the latter at all.

The last two parameters, ε_{sep} and $\varepsilon_{\text{transp}}$, are normally close to unity. Only when a very high mass resolving power ($m/\Delta m > 10000$) is required to provide some isobaric selectivity, one has to accept substantial losses in ε_{sep} .

Equation (1) which looks like a simple product is indeed more complicated since most factors are interdependent. For example, an increase of N by increasing the target length is in principle possible if the energy of the primary beam is high enough to provide a sufficient range,

^a e-mail: Ulli.Koster@cern.ch

¹ See [3] for a popular illustration of this formula.

but it is obvious that a radioactive particle can get easier “lost” and decays before finding its way to the ion source when using a bigger ISOL target, *i.e.* a massive increase of the target size will reduce the release efficiency ϵ_{target} . However, this effect depends strongly on the exact target geometry and the interplay between diffusion and effusion. An optimization of the target size and geometry has in principle to be done individually for every element and isotope and no general relationship between N and ϵ_{target} can be given. To produce intense RIBs the optimization of the parameters in eq. (1) will be discussed in the following. Obviously, the adjective “intense” depends strongly on the isotope under consideration. While ^{80}Rb beams with $\approx 10^{10}$ ions/s are standard at facilities like ISOLDE or ISAC, a ^{74}Rb beam $\geq 10^4$ ions/s became only available recently at ISAC using 20 μA of primary proton beam [4].

3 Primary-beam intensity

The RIB intensity of most existing RIB facilities is limited by the available driver beam intensity. An increase of the final RIB intensity seems to be obvious when using a more powerful primary beam. However, apart from the fact that the primary accelerator needs to be bigger and more expensive, more constraints will be encountered.

3.1 Beam-induced target heating

Charged-particle beams heat the target, *e.g.* 1 GeV protons lose by electronic stopping 80 MeV when passing a standard ISOLDE $\text{UC}_x/\text{graphite}$ target (50 g/cm^2 ^{238}U and 10 g/cm^2 C [5]). Thus, a 100 μA beam would heat the target with² > 8 kW, more than it can stand in its present design. The heating is even worse for lower-energy protons and for projectiles with higher Z .

Special targets were designed to maximize the power they can dissipate by radiation [6]. The RIST target, a Ta foil target which should stand a 800 MeV p beam of up to 100 μA , was successfully tested off-line with 24 kW external heating. For target materials which have to be operated at lower temperatures, radiative cooling is less effective. Conductive cooling with water [7] and liquid lithium [8] was proposed instead. The thermal behaviour of a water-cooled Mo foil target was successfully tested at ISAC with up to 100 μA protons of 500 MeV [9].

3.2 Target lifetime

The yields from ISOLDE targets often drop significantly (factor 3 to 10) after a week or fortnight of continuous operation. The target deterioration is not a simple time effect, since, *e.g.*, at the reactor-based ISOL facility OSIRIS $\text{UC}_x/\text{gr.}$ targets are used without observable

² Additional energy is deposited by nuclear interactions of the beam and the interaction of secondary particles.

degradation over many weeks or even months [10]. However, at ISOLDE the target is directly bombarded by an intense proton beam. During one week of operation with 2 μA the target is exposed to ≈ 1 C of protons in total. If the target ageing were just dose dependent, the same degradation would occur in only three hours with a 100 μA beam. First experiences with Nb targets bombarded at ISAC with over 30 C of protons did not show any deterioration [4]. The particularity at ISOLDE is the very pronounced bunching of the proton beam from the PS Booster synchrotrons: $3 \cdot 10^{13}$ protons are delivered within 2 μs short pulses. The peak current reaches 2.5 A and the peak power density deposited in a $\text{UC}_x/\text{gr.}$ target exceeds 6 MW/cm^3 ! These intense proton bunches are deleterious for the target [11]. Thus, the driver beam of a high-intensity ISOL facility needs to be less bunched, *i.e.* should be as close as possible to cw.

Finally, the number of radioactive nuclei produced inside the ISOL target will always be limited by the maximum beam intensity a target can tolerate. This number varies strongly for different target materials. For a fragile ThO_2 powder target [5] it will be much lower than for a robust graphite [12] or W foil target [13].

3.3 Radioactivity management

In fission or spallation a multitude of different isotopes is produced simultaneously. Thus, for the production of a given amount of one desired exotic isotope, many orders of magnitude more radio-isotopes will be produced in the ISOL target. Even when using a rather selective reaction like thermal-neutron-induced fission to produce, say, $6 \cdot 10^{10}$ atoms/s of ^{132}Sn , the ISOL target will present during operation a radioactive source of ≈ 10 kCi which is necessarily “open” for the release of volatile elements. When bombarding instead a ^{238}U target with a high-energy beam, also spallation products are produced, including ample amounts of volatile α -emitters (Rn, etc.). The safety aspects are important design parameters for a high-intensity ISOL facility, *i.e.* the strong radiation environment during operation, the residual activity after irradiation, the volatile activity deposited in the “front-end” area and the following vacuum system, the radioactive ions deposited in the magnetic separator, etc. [14,15].

3.4 Neutron-induced reactions

Fission is the best-known method to produce neutron-rich medium-mass nuclei. Neutron beams are better to induce fission than charged-particle beams. This reduces simultaneously all three problems mentioned before. The straightforward way is the use of thermal neutrons, available from a reactor. More than a dozen reactor-based RIB facilities have been operating up to now [16] and the MAFF project [17] aiming at 10^{14} fissions/s is under preparation at the high-flux reactor FRM-II in Munich.

Neutron beams can also be produced with a primary beam from an accelerator. Already in the very first ISOL facility [1], a 10 MeV deuteron beam from the cyclotron

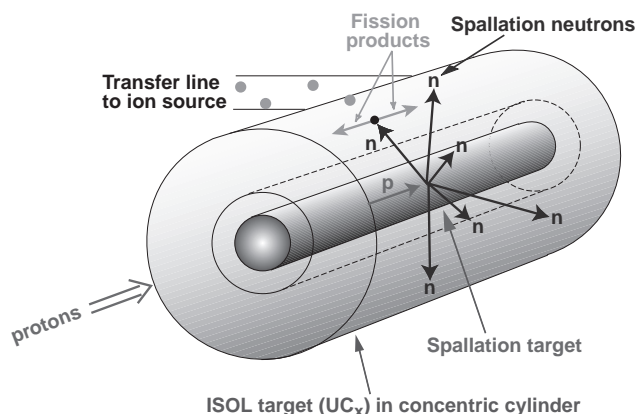


Fig. 1. Scheme of an ISOL target fed by spallation neutrons.

was “converted” via an internal Be target into a neutron beam and only the latter was hitting the uranium-containing ISOL target [18]. The break-up of intense medium-energy ^2H beams to produce fast neutrons and to induce fission in a ^{238}U ISOL target was later proposed by Nolen [19]. The feasibility of this concept was meanwhile studied in detail in the PARRNe project [20, 21].

Spallation of a heavy target with high-energy protons also efficiently produces neutrons [22]. These can be used for many applications: spallation neutron sources, accelerator-driven systems, etc., but also to induce fission in a close-by ISOL target. A compact set-up with a spallation target (called “converter”) of some cm diameter (circulating liquid Pb or liquid-lithium-cooled W [8]) surrounded by a concentric ISOL fission target was first proposed by Nolen *et al.* [23]. Such a mini spallation neutron source for ISOL applications (fig. 1) could reach 10^{14} – 10^{15} fissions/s. More detailed studies are required to optimize the converter and target geometry for efficient use of the neutrons *and* simultaneously efficient release of the created radionuclides.

In fact, it is technically easy to install just a heavy-metal rod (Ta or W) parallel to the standard fission target of an operating ISOL facility. Only part of the neutrons produced in the converter will hit the ISOL target, but it is sufficient to demonstrate the principle and to collect data to validate the simulations. Such experiments were already performed at PNPI-IRIS [24] and ISOLDE [25]. For the most neutron-rich fission products “converter efficiencies” (*i.e.* the yield ratio when directing the proton beam onto the converter or directly onto the ISOL target) of 35% and more were obtained. Keeping in mind that the ISOL target of this test design covers only about 10% of the radial solid angle and that the target thickness in radial direction was only $\approx 3 \text{ g/cm}^2$ ^{238}U at ISOLDE and even less at IRIS, shows that finally (fig. 1) a conversion efficiency of the order of 1000% could be reached.

3.5 Photo-fission

Photo-fission of ^{238}U induced by bremsstrahlung from a medium-energy ($\approx 50 \text{ MeV}$) electron beam was recently

proposed for an ISOL facility [26]. First experiments have shown the feasibility of this method [27, 28]. However, much of the beam energy is deposited in the ISOL target (either by the primary e^- beam or, when using a converter, by pair creation of the secondary γ -rays) while the fission probability per incident e^- is low ($\approx 0.4\%$ for $50 \text{ MeV } e^-$, depending on the target geometry). Thus, the energy deposition per fission will be several GeV, much higher than in all other production scenarios! Therefore, photo-fission might be an economic way (e^- accelerators are inexpensive compared to p or d accelerators) to reach a limited production rate in the ISOL target of, say, 10^{13} fissions/s, but it is difficult to imagine to produce with this method $\gg 10^{14}$ fissions/s in a compact target.

4 Production cross-sections

Since an increase of the production rate by just changing Φ or N is difficult, it is very important to optimize σ .

The energy dependence of σ is particularly high for the production of light fragments from heavy targets in multi-fragmentation and hot fission [29]. Here σ continues to rise till $\approx 10 \text{ GeV}$, see fig. 2. The ratio of σ to the incident proton energy (*i.e.* the “energy costs” to produce a given radio-isotope) reaches a maximum around 4 GeV . The discussed rise of σ does not yet include further enhancement effects via secondary reactions in a thick target, nor the possibility to increase the target length while keeping the Bragg peak of the primary beam outside the target. Both effects will favor the higher-energy projectiles even more. Only few measured σ exist for more short-lived isotopes in this area, but in tests at ISOLDE with 1.0 and 1.4 GeV protons the higher energy provided 2.5 to 5.5 times higher yields for $^{23-28}\text{Ne}$ from a UC_x/gr . target [30]. This indicates that the energy dependence for the exotic isotopes of interest is comparable to, if not more pronounced than³, that of ^{24}Na . Recent investigations at GSI-FRS have shown that with 1 GeV p onto ^{238}U neutron-rich isotopes down to $Z = 10$ are indeed produced in hot fission [32].

Another reaction mechanism which shows a strong rise of σ with energy is deep spallation (subsect. 6.2). On the other hand, close spallation reactions reach maximum σ already at lower energies ($\approx 100 \text{ MeV}$ – 1 GeV). Hence, an ideal driver accelerator for an ISOL facility should be able to provide proton beams of variable energy (in steps) between some hundred MeV and several GeV.

5 ISOL versus fragment separator

ISOLDE and the fragment separator GSI FRS have quite similar beam energies (1.0 or 1.4 GeV protons the former and up to $1 A \cdot \text{GeV}$ the latter), and comparably “thick” targets. To calculate the number of interactions in the

³ Note that the very exotic isotope ^{35}Na was observed only once up to now, produced by 10 GeV protons onto a Ir/graphite target at the CERN PS on-line mass spectrometer [31].

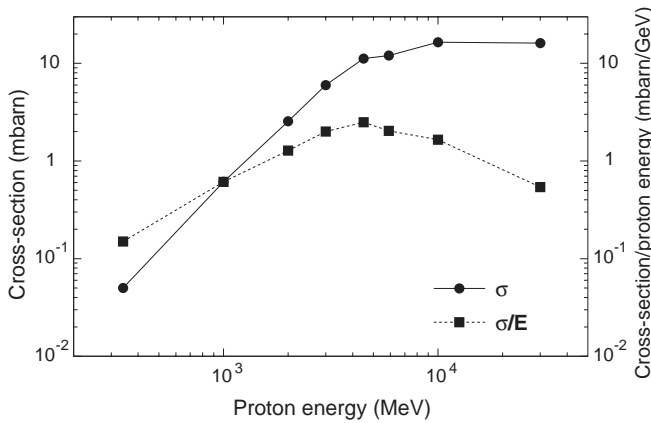


Fig. 2. Experimental cross-sections and “energy costs” for the reaction $^{238}\text{U}(p, X)^{24}\text{Na}$. Data are from [33–35].

target, it is useful to measure its thickness in mol/cm^2 instead of g/cm^2 . ISOLDE targets [36] normally vary from $0.1 \text{ mol}/\text{cm}^2$ (oxides) to $1.5 \text{ mol}/\text{cm}^2$ (molten metals), while at FRS often Be targets of $0.1\text{--}0.5 \text{ mol}/\text{cm}^2$ are used [37, 38].

Hence, if $^4\sigma$ and the product $\varepsilon_{\text{target}} \cdot \varepsilon_{\text{source}} \cdot \varepsilon_{\text{sep}} \cdot \varepsilon_{\text{transp}}$ are comparable in both cases, it is just the primary beam intensity Φ which matters. Thus, in favorable cases, *i.e.* for sufficiently long-lived isotopes where the decay losses are not important ($\varepsilon_{\text{target}} \approx 1$) and the ion source efficiency of the ISOL facility is comparable to the fragment separator transmission, an ISOL facility like ISOLDE can surpass a high-energy fragmentation facility like the FRS by the ratio of the available projectile beam intensities, *i.e.* a factor of $10^4\text{--}10^6$ at present [37, 38]. It will also give more intense beams than the fragmentation facility for all those isotopes where the release losses are smaller than this factor. Depending on the physics application, some more factors have to be added to eq. (1). Where “fast” beams are required, the low-energy ISOL beams need to be post-accelerated and the corresponding losses need to be accounted for. The “charge state breeding” or stripping efficiency, transmission of the accelerator, losses due to a mismatch between the time structure of the beam and the duty cycle of the accelerator, etc. may accumulate to one or two orders of magnitude loss. This will favor the in-flight facilities correspondingly. If, on the other hand, low-energy beams are required, the in-flight facilities are disfavored by a certain loss factor occurring during deceleration of the fast beam. Fragment separators of high-energy beams can directly provide beams spatially separated according to Z when using the different energy loss in a degrader followed by an energy-dispersive element. In an ISOL facility, extra chemically selective stages have to be introduced to perform an isobaric purification.

There is a substantial difference between a fragment separator using projectile fragmentation and an ISOL fa-

cility using target fragmentation. The former can, in principle, use projectile beams of any stable isotope. The latter has only a restricted choice of possible target isotopes:

- 1) Short-lived isotopes cannot be extracted from a target made from the same element (*e.g.*, no ^{100}Sn from a tin target), since at a temperature where the isotope in question is released sufficiently fast, the complete target would be evaporated within short time.
- 2) Several elements are too volatile (in elemental form as well as chemical compounds) to serve as a target, *e.g.* there are obviously no xenon ISOL targets.
- 3) Due to the large required amounts for a target filling (several 10 to 100 g) the cost of isotope-enriched targets (^{48}Ca , ^{112}Sn , etc.) is normally prohibitively expensive for thick-target ISOL facilities.

6 Target and ion source optimization

A detailed discussion of the different ISOL targets and ion sources would go beyond the scope of this article. Overviews can be found, *e.g.*, in [39–41, 36]. In the following just four types of ion sources will be mentioned:

FEBIAD: The Forced Electron Beam Ion Arc Discharge ion source [42] is particularly well adapted for ISOL facilities. It provides good ionization efficiencies (20–70%) for many elements heavier than Ar [43]. Many variants exist, even one with a plasma chamber volume of only 1.3 cm^3 which can be kept at 2300 K [44].

ECRIS: Most Electron Cyclotron Resonance Ion Sources [45] have a relatively large plasma chamber with “cold” walls and are therefore mainly suitable for volatile gases (noble gases, CO, N_2 , etc.). The ECRIS allows to reach high ion source efficiencies (*e.g.*, 90% for Ar^+ [46]) even for light atoms and molecules with high ionization potential (He, Ne, Ar, etc.). It can also produce efficiently multiply charged ions.

Surface ion source: Elements with low ionization potential can be positively ionized by an interaction with a hot surface of high work function (*e.g.*, noble metals). Alkalis and some other elements are selectively ionized with high efficiency (some % up to 100%) [47].

RILIS: The Resonance Ionization Laser Ion Source provides a chemically selective way to excite the valence electron of a given element by resonant absorption of laser light via two or three steps into the continuum. This works particularly well for metallic elements. Ionization schemes for 21 different elements were tested up to now at ISOLDE providing ionization efficiencies of some % to some ten % [48]. Due to the different hyperfine splitting of certain isomers even isomerically “pure” beams can be produced with the RILIS [49].

While new ISOL facilities often start out with a limited number of available beams (*e.g.*, only alkalis at ISAC and only noble gases at SPIRAL), in the long run the diversity of beams it can provide will be an important asset for every RIB facility. Thus, new ISOL beams need to be developed, *i.e.* the parameters of eq. (1), in particular

⁴ This is not exactly the case, since H_2 targets are used at the FRS mainly for cross-section measurements [32] while the Be targets used for production purposes give a higher excitation energy to the projectile (9 GeV ^9Be versus 1.4 GeV p).

$\varepsilon_{\text{target}}$ and $\varepsilon_{\text{source}}$, need to be optimized for an individual element or isotope. The status of such beam developments will be discussed for the examples of O, In and Ga.

6.1 Oxygen beams

The first ISOL beams of oxygen (10^3 – 10^4 ions/s of ^{15}O) were produced at LISOL (Leuven) via (α, n) reactions in the graphite catcher of a FEBIAD ion source [50]. Graphite is a favorable material for oxygen release since it allows the formation of the volatile gases CO and CO_2 . Later a dedicated beam development was made where $^{14,15}\text{O}$ were produced in graphite targets via $(^3\text{He}, n)$ and (α, n) reactions, respectively [51] and then ionized with FEBIAD and ECRIS [52]. The FEBIAD provides very clean $^{12}\text{C}^{14}\text{O}^+$ beams of up to $2.3 \cdot 10^5$ ions/ μC of primary ^3He beam, though the total efficiency is only $\varepsilon_{\text{target}} \cdot \varepsilon_{\text{source}} = 0.4\%$ [53]. Since at CRC Louvain-la-Neuve the available p beams are much more intense than the α beams, ^{15}O is now produced via $^{19}\text{F}(p, \alpha n)$ reactions in liquid LiF (held in a graphite matrix). Here, a release efficiency of up to $\varepsilon_{\text{target}} = 24\%$ and an on-line ionization efficiency of the ECRIS for 2+ ions of $\approx 5\%$ were obtained [54]. This gives an impressive beam of $1.4 \cdot 10^{10}$ $^{15}\text{O}^{2+}$ ions/s with 300 μA of 30 MeV p onto the target.

In 1990 $^{19-22}\text{O}$ were produced at ISOLDE-SC from a Pt/graphite powder target [55] and extracted as CO^+ beams, but the efficiency was rather low: $\varepsilon_{\text{target}} \cdot \varepsilon_{\text{source}} \approx 0.02\%$. A special FEBIAD ion source made from graphite and equipped with a W cathode⁵ was used. The ionization efficiency was generally low (only 0.3% for stable Ne). It should be possible to enhance the O yields significantly by using instead a dedicated ECRIS.

^{14}O beams were recently developed at LBL in the frame of the BEARS [56] and IRIS [57] projects. Originally, the set-up was tested with ^{14}O produced via (p, n) reactions in a N_2 gas target, but now a carbon aerogel target is used for production of ^{14}O via $(^3\text{He}, n)$ reactions. Up to now, beams of up to $3 \cdot 10^7$ $^{14}\text{O}^+$ /s were obtained with $\varepsilon_{\text{target}} = 46(5)\%$ and $\varepsilon_{\text{source}} \approx 4.3\%$ [57]. Also a $^{14}\text{O}^{6+}$ beam was produced with the AECR-U source ($\varepsilon_{\text{source}} = 3.6\%$) [58] and accelerated with the 88 inch cyclotron [59].

$^{14,15}\text{O}$ beams were also produced at SIRa (GANIL) [60]. The standard SPIRAL graphite target [12] serves here as fragmentation target of an incident ^{16}O beam (95-A MeV), see fig. 3. With the Nanogan-III ECRIS $\varepsilon_{\text{target}} \cdot \varepsilon_{\text{source}} = 4.6\%$ was obtained for $^{14}\text{O}^+$ [60]. Note that, when fragmenting the projectile, the target element can be chosen rather independently to optimize the release properties without observing the constraint $(A, Z)_{\text{target}} > (A, Z)_{\text{product}}$. Also beams of $^{19-22}\text{O}$ were produced at SIRa by fragmenting a 76-A MeV ^{36}S beam in a graphite target placed inside the SHyPIE ECRIS [61].

⁵ In a standard ISOLDE FEBIAD ion source the cathode is made from Ta which will act at high temperatures as efficient getter for the reactive oxygen. Graphite does not cause this problem, but the W cathode can still act as getter.

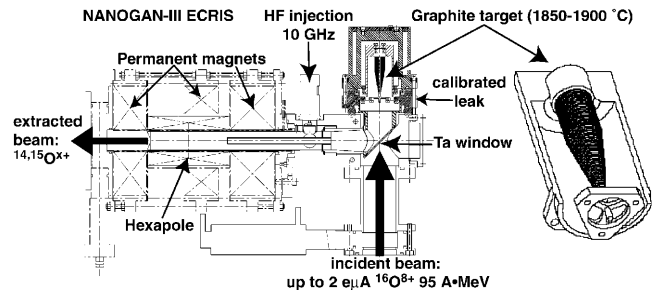


Fig. 3. Production of $^{14,15}\text{O}$ beams at SIRa and SPIRAL.

A very intense ^{15}O beam ($\sim 10^{11}$ ions/s) still needs to be developed at ISAC (TRIUMF) to fulfill the ambitious intensity requirements for a measurement of the $^{15}\text{O}(\alpha, \gamma)^{19}\text{Ne}$ reaction at astrophysical energies with the DRAGON facility [62].

It should be noted that the various source efficiencies mentioned in this paragraph are not directly comparable since the ion sources were optimized for different charge states and beam purity depending on the further application (post-acceleration, etc.).

6.2 Neutron-deficient indium beams

Neutron-deficient In isotopes were produced at ISOLDE from a $\text{LaC}_x/\text{graphite}$ (≈ 30 g/cm² La) target with a W surface ionizer. The In yields were measured with three different proton beam energies: 0.6 GeV, 1.0 GeV and 1.4 GeV, see fig. 4. With each increase in energy the yields of the most exotic isotopes rise by nearly one order of magnitude. Finally, the ionization efficiency was enhanced by $\approx 60\%$ when using instead of pure surface ionization additionally the RILIS which was tuned to excite indium in two steps: with a frequency-doubled dye laser beam of 303.9 nm from the $^2P_{1/2}^o$ atomic ground state to the $^2D_{3/2}^o$ excited state and then with the green and yellow copper vapor laser beams (511 and 578 nm) non-resonantly to the continuum. This excitation scheme had been developed in

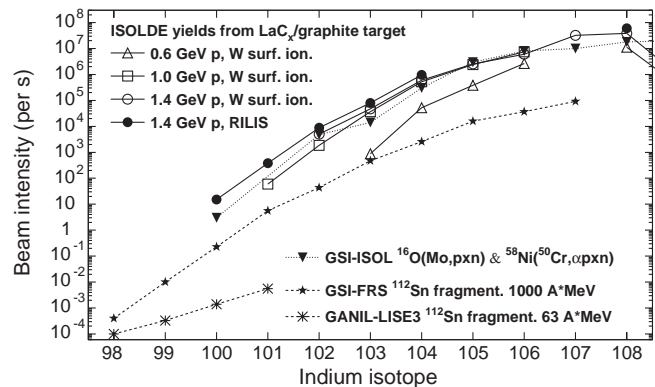


Fig. 4. Beam intensities of neutron-deficient In isotopes measured at ISOLDE, GSI-ISOL [63–65], LISE3 [66] and FRS [38]. The ISOLDE intensities are given for 2 μA of proton beam. In cases where several isomers exist, their sum yield is shown.

Troitsk [67]. The absolute ion source efficiency for indium was estimated to $\sim 10\%$. With an optimized RILIS set-up it could be further improved by a factor 2 to 3.

With the target at $1850\text{ }^\circ\text{C}$ and the W ionizer at $2300\text{ }^\circ\text{C}$ the release efficiency for In isotopes with $> 5\text{ s}$ half-life was $\varepsilon_{\text{target}} > 85\%$, hence the shown beam intensities of $^{100-108}\text{In}$ directly reflect the relative behaviour of the cross-sections.

GSI-ISOL has a long-standing tradition in producing neutron-deficient In beams in fusion-evaporation reactions. Their intensities are quite comparable to the ISOLDE ones, see fig. 4. Recently, a detailed ^{100}In decay study was performed [68]. ^{100}In was produced via $^{50}\text{Cr}(^{58}\text{Ni}, \alpha p3n)$ and thermally ionized in a W ionizer. With a $45\text{ pA } ^{58}\text{Ni}$ beam 5 ions/s of ^{100}In were produced.

While at the fragment separators LISE3 and FRS ^{98}In could be clearly identified [66,38], with an ISOL facility it would be very difficult to detect such a low yield among the isobaric background. The problem is here rather insufficient selectivity than insufficient efficiency.

Isotopes close to ^{100}Sn are generally difficult to produce by spallation in a thick-target ISOL facility. The next-closest elements Sb to Cs do not form very stable compounds which could be heated to high temperatures and serve as an ISOL target. Ba, La and heavier lanthanides can be used as target, but then very high proton energies ($\gg 1\text{ GeV}$) are required to obtain reasonable production cross-sections in deep spallation. When using high-energy spallation reactions, the large number of different nuclides produced from a single target is quite useful since it allows to use the same target for a multitude of different beams. However, this fact is not always a blessing, but may also become a curse.

In an earlier ISOLDE experiment neutron-deficient Cd isotopes were produced with the same $\text{LaC}_x/\text{gr.}$ target mentioned above and ionized with the RILIS [69]. When searching for γ -rays following the β -decay of a ^{97}Cd isomer indeed γ -rays with a short half-life were observed. Unfortunately, they were also present in the “laser-off” background spectrum, *i.e.* they must belong to a surface ionized isobar. However, the elements neighboring Cd have a rather high ionization potential and the only isobar on mass 97 with a really low ionization potential is Rb. In fact the γ -rays belonged to the decay of ^{97}Rb and its decay daughters. At first glance it is very surprising that a β -delayed neutron emitter is observed when a β -delayed proton emitter was searched for. Figure 5 shows $\sigma_{\text{spallation}}$ calculated with the semi-empiric model of Silberberg and Tsao [70]. Indeed more ^{97}Rb is produced in the target than ^{97}Cd . In comparison are shown $\sigma_{\text{fusion-evaporation}}$ for the reaction $^{40}\text{Ca}(^{60}\text{Ni}, x)^{97}\text{X}$ used for the production of ^{97}Cd at GSI-ISOL. These were calculated with the HIVAP code [71]. The huge difference in σ is partly compensated by the higher target thickness ($3000\times$) and the higher primary beam intensity ($50\times$) at ISOLDE. Thus the final RIB intensity is in the same order of magnitude, but there is an important difference in the intrinsic beam purity: while in this fusion-evaporation reaction $A = 97$ isobars with $Z \leq 45$ cannot be produced from the ^{100}Cd com-

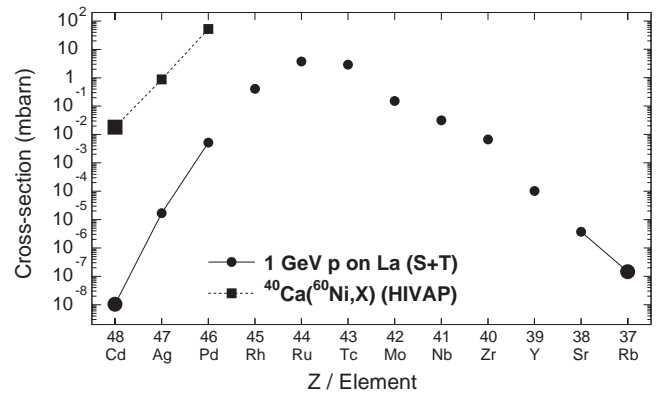


Fig. 5. Calculated⁶ production cross-sections for $A = 97$ isobars.

pound nucleus, in the case of spallation nine more isobars are present. The elements with $Z = 40\text{--}46$ are rather refractory and are not supposed to be released significantly from the $\text{LaC}_x/\text{gr.}$ target at $1850\text{ }^\circ\text{C}$, but ^{97}Rb is easily released and ionized. It needs to be removed by an additional chemical selective step.

Note that the discussed effect is a general feature of all steps of the separation process: *an increased universality has normally to be paid for with a loss in selectivity!*

6.3 Neutron-rich gallium beams

A similar problem of isobaric contaminations occurs when studying neutron-rich isotopes produced in high-energy proton-induced fission. In the same target neutron-deficient isobars will be produced by spallation and high-energy fission. The situation is particularly bad around masses 80 and 130, where the interesting exotic isotopes are covered by an order of magnitude higher background of the difficult-to-suppress isobars Rb and Cs, respectively.

The half-lives of $^{79-84}\text{Ga}$ were already studied by detection of β -delayed neutrons at ISOLDE [72], but the enormous background of neutron-deficient Rb isotopes made a detailed $\beta\gamma$ spectroscopy rather difficult. With a 1.4 GeV proton beam onto a $\text{UC}_x/\text{gr.}$ target the ^{82}Rb background is above $10^8\text{ ions}/\mu\text{C}$, *i.e.* about two orders of magnitude more intense than the ^{82}Ga yield! Even with an optimized timecycle (implantation, measurement, removal of long-lived activity with a tape transport) the Rb background is disturbing and for heavier masses the Rb/Ga ratio is even worse. Obviously, the ultimate beam purity would be achieved when combining the selective production method of thermal-neutron-induced fission⁷ with the selective and efficient RILIS. This is foreseen for the next-generation facility MAFF, but the use of the converter target discussed

⁶ The real cross-sections might differ from the calculated ones by an order of magnitude or more, but for the purpose of illustration the calculated ones do their job.

⁷ Only upper limits exist for the yields of neutron-deficient isotopes produced in low-energy fission, but they are far below the 10^{-7} level [73].

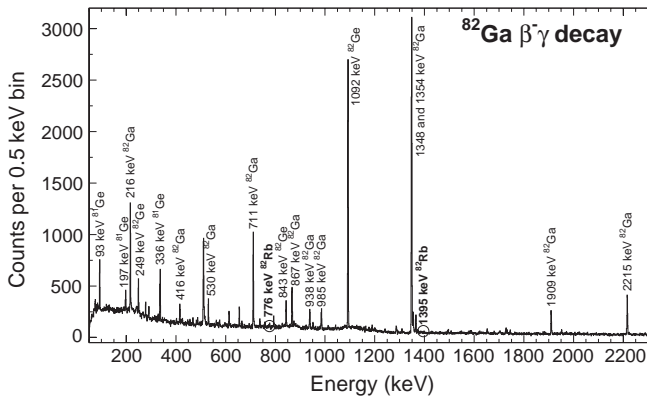


Fig. 6. Spectrum of the ^{82}Ga β^- - γ -decay taken with an ISOLDE beam produced from a UC_x /graphite target with a “converter” and the RILIS tuned for Ga ionization. Note the absence of any disturbing ^{82}Rb contamination.

in subsect. 3.4 allows to use neutron-induced fission also at the existing ISOL facilities equipped with a high-energy proton driver. The gain in selectivity is not perfect since part of the primary and secondary high-energy particles still hit the close-by target, but it can be further optimized by adapting the geometry.

Ga was ionized with a RILIS scheme [74] similar to In: with a frequency-doubled dye laser beam of 287.4 nm from the $^2P_{1/2}^o$ atomic ground state to the $^2D_{3/2}^o$ excited state and then with the green and yellow copper vapor laser beams non-resonantly to the continuum. Off-line it had been measured that the RILIS can enhance the Ga ionization efficiency from $\approx 0.7\%$ (2150 °C W surface ionizer) to $\approx 20\%$. On-line the RILIS gives not only an increased yield⁸, but provides moreover the possibility to identify weak γ -rays as being related to the Ga decay by comparing “laser-on” and “laser-off” spectra. Figure 6 shows a β -gated γ -ray spectrum of the ^{82}Ga decay. The release profile measured with both, target and Nb cavity, at 2100 °C shows that the release efficiency $\varepsilon_{\text{target}}$ drops from 90% for 13 s ^{77}Ga , to 50% for 1.2 s ^{81}Ga and to $\approx 7\%$ for 85 ms ^{84}Ga .

Figure 7 shows Ga yields measured with a standard ISOLDE UC_x /gr. target by direct proton bombardment and when using the “converter”. For comparison the yields measured at OSIRIS⁹ [75, 76], IGISOL [77] and FRS [37] are also shown. Obviously, the IGISOL and FRS yields are much lower due to the thinner target or lower primary beam intensity, respectively. However, their “extraction efficiency” ($\varepsilon_{\text{target}} \cdot \varepsilon_{\text{source}}$) is rather element independent. Thus, these methods are particularly suitable for the production of RIBs from “refractory” elements which are difficult to produce with the standard ISOL technique.

⁸ Also in this short test the RILIS efficiency was lower than normally and the given yields should be seen as a lower limit for real operation conditions.

⁹ These beam intensities were calculated from the relative yields of [75] and scaled with the absolute yield of [76].

¹⁰ *Additional remark:* In a target inspection after the experiment it was observed that the Ta converter got strongly bent.

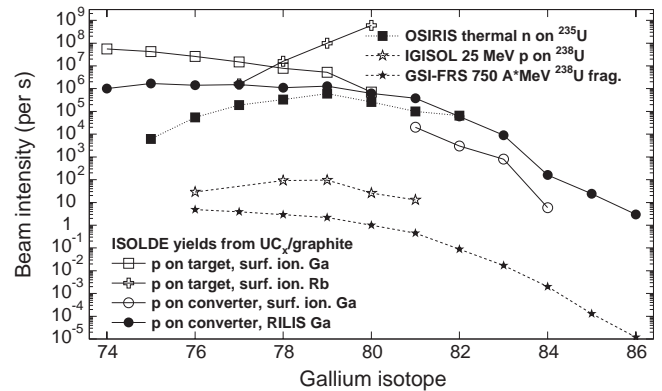


Fig. 7. Beam intensities of neutron-rich Ga isotopes measured at ISOLDE, OSIRIS, IGISOL and FRS. For ISOLDE are shown the production of Ga and Rb by direct proton bombardment and of Ga when using the “converter”¹⁰.

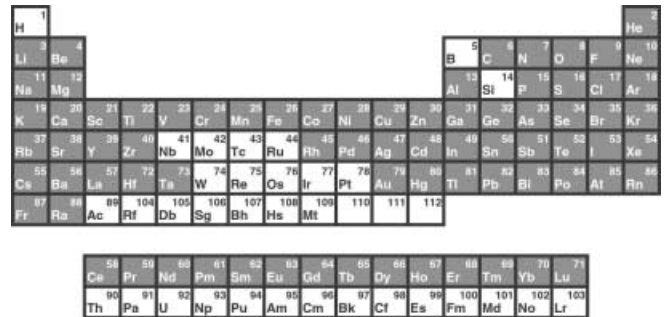


Fig. 8. Elements which have been produced as ISOL beams.

7 Conclusions

Figure 8 shows which of the chemical elements have already been produced as ISOL beams. This combines the ISOLDE SC beams [55], unpublished results of ISOLDE PSB (for S, Cr and Co beams), and the elements available at GSI ISOL [78, 65]. In a test at SIRa beams of radioactive P and S isotopes were observed [79]. Even ISOL beams of rather short-lived isotopes (in the s to min range) of the refractory elements Zr and Ta were produced with a dedicated technique at ISOCELE already 20 years ago [80]. Obviously many of these beams are not yet optimized in efficiency, rapidity or selectivity, but at least the release of some longer-lived isotopes was already observed.

For medium heavy nuclides close to the proton dripline the beam intensities provided from present thick-target ISOL facilities like ISOLDE and thin-target facilities like GSI-ISOL are often similar within one order of magnitude. While the former is favored for elements with good release characteristics (*e.g.*, Kr), the latter often provides a higher intrinsic beam purity due to a more selective production reaction.

In-flight facilities can work with fixed energy and different projectiles, but a high-energy proton-driven ISOL facility has a reduced choice of possible target elements

Thus the presented yields are considerably lower compared to a normal straight converter.

and profits strongly from a variable proton energy to optimize the production cross-sections for individual isotopes.

It has been shown that ISOL facilities already now provide intense beams of many elements. However, there are still “white spots” on the periodic table which were not yet accessed. *This does not at all mean that such beams cannot be produced, but just that up to now nobody made sufficient effort to design a suitable ISOL system.* In principle, ISOL beams could be created for every element, though with varying efficiency, in particular when considering short-lived nuclei. The production of beams of a refractory element, *e.g.* Os, is probably possible by using a molecular technique (OsO₄ is extremely volatile [81]), but before coming to an on-line use one needs to adapt the target container, the transfer line and the ion source to cope with large amounts of carrier gas (here O₂) and to maintain all pieces at a suitable temperature. Thus, the tedious development of new ISOL beams of refractory elements might take longer than many users accept to wait. Often either they develop themselves clever techniques to circumvent the problem (*e.g.*, the COMPLIS set-up [82] is used for laser spectroscopy of Au, Pt and Ir isotopes populated in the decay of easily available Hg beams) or they study a similar physics problem with already available beams.

The IGISOL technique provides excellent beams of short-lived nuclides (even below 1 ms half-life [83]), also of refractory elements. However, it is difficult to produce very intense beams with this method. Too intense primary or secondary beams can induce a plasma in the gas cell which will prevent a rapid and efficient extraction of the produced radio-isotopes. This “plasma-effect” is discussed in detail in [84]. Moreover, it is more difficult to handle large amounts of radioactivity in the extensive gas circulation system of an IGISOL set-up than with a solid ISOL target where the major part of the radioactivity will be condensed close to the target. Presently, big hopes are put into a combination of an in-flight separator and an IGISOL set-up in series to profit from the advantages of both methods: SHIPTRAP [85], RIA [86], etc. A similar breakthrough could be achieved by combining in an optimized way chemical on-line separators with the ISOL method. The chemical separators provide both, a good efficiency and a very good chemical selectivity. The EU RTD project TARGISOL will make an extensive data collection of diffusion and desorption parameters. This is an important requirement for a future systematic optimization of ISOL target and ion source units with respect to release efficiency and chemical selectivity.

Thanks to Stéphane Gibouin for communicating the results of the SIRa ¹⁴O release test, to Jason Burke for the results from IRIS, to the TAGS Collaboration for using their set-up during the yield test of neutron-deficient In isotopes, to Einar Hagebø for various cross-section calculations, to Reinhard Kirchner for the HIVAP cross-sections (fig. 5), and to the IS365 Collaboration for the ⁸²Ga decay spectrum (fig. 6). Several of the presented ideas were born or extended during discussions in

the frame of the EU-RTD project EURISOL (contract HPRI-CT-1999-50001).

References

1. O. Kofoed-Hansen, K.O. Nielsen, *Mat. Fys. Medd. Dan. Vid. Selsk.* **26**, 1 (1951).
2. D. Forkel-Wirth, G. Bollen (Editors), *ISOLDE – a laboratory portrait*, *Hyperfine Interact.* **129** (2000).
3. U. Köster, *Prog. Part. Nucl. Phys.* **46**, 411 (2001).
4. G.C. Ball *et al.*, *Phys. Rev. Lett.* **86**, 1454 (2001).
5. H.L. Ravn *et al.*, *Nucl. Instrum. Methods B* **26**, 183 (1987).
6. J.R.J. Bennett, *Nucl. Instrum. Methods B* **126**, 105 (1997).
7. W.L. Talbert *et al.*, *Nucl. Phys. A* **701**, 303 (2002).
8. J.A. Nolen *et al.*, *Nucl. Phys. A* **701**, 312 (2002).
9. P. Bricault, in *CAARI 16*, edited by J.L. Duggan, I.L. Morgan, *AIP Conf. Proc.* **576**, 239 (2000).
10. B. Fogelberg *et al.*, in *Research with Fission Fragments*, edited by T. von Egidy *et al.* (World Scientific, 1997) pp. 69-73.
11. J. Lettry *et al.*, *Nucl. Instrum. Methods B* **126**, 170 (1997).
12. J.C. Putaux *et al.*, *Nucl. Instrum. Methods B* **126**, 113 (1997).
13. V.N. Panteleev *et al.*, *Nucl. Phys. A* **701**, 470 (2002).
14. J.A. Pinston, *Nucl. Instrum. Methods B* **126**, 22 (1997).
15. P.W. Schmor, *Nucl. Phys. A* **701**, 480 (2002).
16. U. Köster *et al.*, in *Research with Fission Fragments*, edited by T. von Egidy *et al.* (World Scientific, 1997) pp. 29-40.
17. T. von Egidy *et al.*, *Acta Phys. Slovaca* **49**, 107 (1999).
18. O. Kofoed-Hansen, in *3rd International Conference on Nuclei far from Stability, Cargèse* (CERN 76-13, Geneva, 1976) pp. 65-70.
19. J.A. Nolen, in *RNB 3*, edited by D.J. Morrissey (Editions Frontières, Gif-sur-Yvette, 1993) pp. 111-114.
20. F. Clapier *et al.*, *Phys. Rev. ST Accel. Beams* **1**, 013501 (1998).
21. S. Kandri-Rody *et al.*, *Nucl. Instrum. Methods B* **160**, 1 (2000).
22. G.S. Bauer, *Nucl. Instrum. Methods A* **463**, 505 (2001).
23. J.A. Nolen *et al.*, in *HIAT'98*, edited by K.W. Shepard, *AIP Conf. Proc.* **473**, 477 (1998).
24. V.N. Panteleev *et al.*, *High temperature uranium carbide targets*, poster contribution, to be published in *Exotic Nuclei and Atomic Masses* (Springer-Verlag, Heidelberg, 2002).
25. R. Catherall *et al.*, *Measurement of the production cross-sections of neutrino-rich Kr and Xe isotopes*, poster contribution, to be published in *Exotic Nuclei and Atomic Masses* (Springer-Verlag, Heidelberg, 2002).
26. W.T. Diamond, *Nucl. Instrum. Methods A* **432**, 471 (1999).
27. Yu.Ts. Oganessian *et al.*, *Nucl. Phys. A* **701**, 87 (2002).
28. F. Ibrahim *et al.*, to be published in *Eur. Phys. J. A* (2002).
29. M. Gloris *et al.*, *Nucl. Instrum. Methods A* **463**, 593 (2001).
30. U. Georg *et al.*, *Nucl. Phys. A* **701**, 137 (2002).
31. M. Langevin *et al.*, *Phys. Lett. B* **125**, 116 (1983).
32. M.V. Ricciardi *et al.*, *Nucl. Phys. A* **701**, 156 (2002).
33. R.L. Folger *et al.*, *Phys. Rev.* **98**, 107 (1955).
34. A.A. Caretto *et al.*, *Phys. Rev.* **110**, 1130 (1958).

35. J. Hudis, S. Tanaka, *Phys. Rev.* **171**, 1297 (1968).
36. U. Köster for the ISOLDE Collaboration, *Radiochim. Acta* **89**, 749 (2001).
37. C.O. Engelmann, PhD Thesis, Tübingen University (1998).
38. A. Stolz, PhD Thesis, TU München (2001).
39. *Proceedings EMIS 11*, Nucl. Instrum. Methods B **26** (1987).
40. *Proceedings EMIS 12*, Nucl. Instrum. Methods B **70** (1992).
41. *Proceedings EMIS 13*, Nucl. Instrum. Methods B **126** (1997).
42. R. Kirchner, E. Roeckl, Nucl. Instrum. Methods **133**, 187 (1976).
43. R. Kirchner, *Rev. Sci. Instrum.* **67**, 928 (1996).
44. R. Kirchner *et al.*, Nucl. Instrum. Methods B **70**, 56 (1992).
45. R. Geller, *Electron Cyclotron Resonance Ion Sources and ECR Plasmas* (IOP, Bristol, 1996).
46. A.C.C. Villari *et al.*, in *CAARI 16*, edited by J.L. Duggan, I.L. Morgan, AIP Conf. Proc. **576**, 254 (2000).
47. R. Kirchner, Nucl. Instrum. Methods A **292**, 203 (1990).
48. U. Köster, Nucl. Phys. A **701**, 441 (2002).
49. U. Köster *et al.*, *Hyperfine Interact.* **127**, 417 (2000).
50. N. Severijns *et al.*, *Phys. Rev. Lett.* **63**, 1050 (1989).
51. M. Gaelens *et al.*, Nucl. Instrum. Methods B **126**, 125 (1997).
52. M. Gaelens *et al.*, in *CAARI 15*, edited by J.L. Duggan, I.L. Morgan, AIP Conf. Proc. **475**, 305 (1998).
53. M. Gaelens *et al.*, *Eur. Phys. J. A* **11**, 413 (2001).
54. M. Loiselet *et al.*, in *CAARI 16*, edited by J.L. Duggan, I.L. Morgan, AIP Conf. Proc. **576**, 269 (2000).
55. <http://www.cern.ch/ISOLDE/normal/isoprodsc.html>.
56. J. Powell *et al.*, Nucl. Instrum. Methods A **455**, 452 (2000).
57. J.T. Burke *et al.*, submitted to *Rev. Sci. Instrum.* (2002).
58. Z.Q. Xie *et al.*, Nucl. Instrum. Methods B **168**, 117 (2000).
59. D. Wutte, LBL, private communication.
60. S. Gibouin, PhD Thesis, Université de Caen (2002).
61. N. Lecesne *et al.*, Nucl. Instrum. Methods B **126**, 141 (1997).
62. J. D'Auria for the DRAGON Collaboration, *Nuclear Astrophysics at ISAC with DRAGON*, to be published in *Exotic Nuclei and Atomic Masses* (Springer-Verlag, Heidelberg, 2002).
63. J. Eberz *et al.*, *Z. Phys. A* **326**, 121 (1987).
64. J. Szerypo *et al.*, *Z. Phys. A* **359**, 117 (1997).
65. K. Schmidt *et al.*, Nucl. Phys. A **701**, 115 (2002).
66. K. Rykaczewski *et al.*, *Phys. Rev. C* **52**, R2310 (1995).
67. M.L. Muchnik *et al.*, *Sov. J. Quantum Electron.* **13**, 1515 (1983).
68. J. Döring *et al.*, GSI scientific report 2000, p. 9.
69. U. Köster, PhD Thesis, TU München (2000).
70. R. Silberberg, C.H. Tsao, *Phys. Rep.* **191**, 351 (1990).
71. W. Reisdorf, *Z. Phys. A* **300**, 227 (1981).
72. K.L. Kratz *et al.*, *Z. Phys. A* **340**, 419 (1991).
73. A.C. Wahl, *At. Data Nucl. Data Tables* **39**, 1 (1988).
74. A.N. Zherikhin *et al.*, *Appl. Phys. B* **30**, 47 (1983).
75. G. Rudstam *et al.*, *Radiochim. Acta* **49**, 155 (1990).
76. B. Fogelberg *et al.*, Nucl. Instrum. Methods B **70**, 137 (1992).
77. M. Huhta *et al.*, Nucl. Instrum. Methods B **126**, 201 (1997).
78. <http://www-aix.gsi.de/~msep/ionsource.html>.
79. N. Lecesne, PhD Thesis, Université de Caen (1997).
80. C.F. Liang *et al.*, *Z. Phys. A* **309**, 185 (1982).
81. A. Türler, this issue, p. 271.
82. J. Sauvage *et al.*, *Hyperfine Interact.* **129**, 303 (2000).
83. J. Äystö, Nucl. Phys. A **693**, 477 (2001).
84. M. Huyse *et al.*, Nucl. Instrum. Methods B **187**, 535 (2002).
85. J. Dilling *et al.*, *Hyperfine Interact.* **127**, 491 (2000).
86. D.J. Morrissey, this issue, p. 105.